Time-Frequency Training OFDM with High Spectral Efficiency and Reliable Performance in High Speed Environments

Linglong Dai, Zhaocheng Wang, *Senior Member, IEEE*, and Zhixing Yang, *Senior Member, IEEE*

***Abstract*—Orthogonal frequency division multiplexing (OFDM) is widely recognized as the key technology for the next generation broadband wireless communication (BWC) systems. Besides high spectral efficiency, reliable performance over fast fading channels is becoming more and more important for OFDM-based BWC systems, especially when high speed cars, trains and subways are playing an increasingly indispensable role in our daily life. The time domain synchronous OFDM (TDS-OFDM) has higher spectral efficiency than the standard cyclic prefix OFDM (CP-OFDM), but suffers from severe performance loss over high speed mobile channels since the required iterative interference cancellation between the training sequence (TS) and the OFDM data block. In this paper, a fundamentally distinct OFDM-based transmission scheme called time-frequency training OFDM (TFT-OFDM) is proposed, whereby every TFT-OFDM symbol has training information both in the time and frequency domains. Unlike TDS-OFDM or CP-OFDM where the channel estimation is solely dependent on either time-domain TS or frequency-domain pilots, the joint time-frequency channel estimation for TFT-OFDM utilizes the time-domain TS without interference cancellation to merely acquire the path delay information of the channel, while the path coefficients are estimated by using the frequency-domain grouped pilots. The redundant grouped pilots only occupy about 3% of the total subcarriers, thus TFT-OFDM still has much higher spectral efficiency than CP-OFDM by about 8.5% in typical applications. Simulation results also demonstrate that TFT-OFDM outperforms CP-OFDM and TDS-OFDM in high speed mobile environments.**

***Index Terms*—Orthogonal frequency division multiplexing (OFDM), time-frequency training (TFT), joint time-frequency channel estimation, interference cancellation, spectral efficiency, fast fading channels.**

I. Introduction

DUE to the robustness to the frequency-selective multipath channel and the low complexity of the frequency-domain equalizer, orthogonal frequency division multiplexing (OFDM) has been widely recognized as one of the key techniques for the next generation broadband wireless communication (BWC) systems [1].

Manuscript received 3 May 2011; revised 29 October 2011. Part of this paper was presented at IEEE Global Communications Conference (GLOBECOM), Houston, Texas, USA, December 2011. This work was supported by National Nature Science Foundation of China (NSFC) under grant No. 61021001 and 60902003, as well as Ph.D. Programs Foundation of Ministry of Education of China under Grant No. 20090002120026.

The authors are with Department of Electronic Engineering as well as Tsinghua National Laboratory of Information Science and Technology (TNList), Tsinghua University, Beijing 100084, P. R. China (e-mails: {daill, zcwang, yangzhx}@tsinghua.edu.cn).

Digital Object Identifier 10.1109/JSAC.2012.120504.

One fundamental issue of OFDM is the block transmission scheme. Basically, there are three types of OFDM-based block transmission schemes: cyclic prefix OFDM (CP-OFDM) [2], zero padding OFDM (ZP-OFDM) [3], and time domain synchronous OFDM (TDS-OFDM) [4]. The broadly used CP-OFDM scheme utilizes the CP to eliminate the inter-block-interference (IBI) as well as the inter-carrier-interference (ICI) [5]. The CP is replaced by zero samples in ZP-OFDM to deal with the channel null problem and improve the equalization performance [3], [6]. For both the CP-OFDM and ZP-OFDM schemes, some dedicated frequency-domain pilots are required for synchronization and channel estimation, thus the spectral efficiency is reduced. To solve this problem, instead of the CP, the known training sequence (TS) such as the pseudorandom noise (PN) sequence, is used as the guard interval in the TDS-OFDM scheme [4]. Since the TS is known to the receiver, it can be also used for synchronization as well as channel estimation [7]. Consequently, the large amount of frequency-domain pilots used in CP-OFDM and ZP-OFDM could be saved. Thus, TDS-OFDM outperforms CP-OFDM and ZP-OFDM in spectral efficiency by about 10% [8]. As the key technology, TDS-OFDM has been successfully adopted by Chinese national digital television standard [9], whose performance has been extensively investigated and verified in China, Hong Kong, South America, etc. [4], [8].

However, the main drawback of TDS-OFDM is that, the time-domain TS and the OFDM data block will cause IBI to each other. Thus, the iterative interference cancellation algorithm has to be used for channel estimation and equalization [7], [8], i.e., the IBI from the OFDM data block to the TS must be eliminated before the TS-based time-domain channel estimation, while the IBI caused by the TS to the OFDM data has to be removed to achieve reliable channel equalization. On one hand, the interference cancellation before channel estimation needs the equalized OFDM data information to calculate the IBI caused by the OFDM block, while on the other hand, channel estimation is prerequisite to obtain the equalized OFDM block. Therefore, channel estimation and channel equalization are mutually conditional in TDS-OFDM, and the iterative interference cancellation algorithm would suffer from high complexity as well as poor performance over fast fading channels [10]. Some alternative solutions have been proposed either to decrease the complexity or to enhance the performance [11], [12], but the performance gain is not obvious. One exciting solution to the interference problem of

0733-8716/12/$25.00 © 2012 IEEE

TDS-OFDM is the cyclic postfix OFDM scheme [13], [14], whereby the TS serving as the cyclic postfix is not independent of the OFDM block like that in TDS-OFDM, but is generated by the redundant frequency-domain comb-type pilots within the OFDM symbol. In this way, the IBI from the TS to the OFDM data block can be avoided. However, the cyclic postfix OFDM scheme does not solve the problem of the interference from the OFDM data block to the next TS, thus the iterative interference cancellation with poor performance over fast time-varying channels is still required for channel estimation and OFDM equalization [15]. In addition, the inserted redundant pilots have much higher average power than the normal OFDM data [16], thus the equivalent signal-to-noise ratio (SNR) at the receiver will be reduced if the identical transmitted signal power is permitted. Such SNR loss can be slightly alleviated by changing the positions of the redundant pilots or adding more pilots in the frequency domain [17], [18], but the effect is not obvious. The most effective solution to the interference problem of TDS-OFDM is to duplicate the TS twice, resulting in the dual-PN OFDM (DPN-OFDM) scheme [19]. The second received PN sequence immune from the interference caused by the preceding OFDM data block can be directly used for channel estimation, and the interference cancellation before channel equalization can be replaced by the cyclic prefix reconstruction which is accomplished by the simple add-subtraction operation [19]. In this way, the iterative interference cancellation algorithm could be avoided, leading to the reduced complexity and improved performance over fast fading channels. However, the spectral efficiency of the DPN-OFDM solution is remarkably decreased by the doubled length of the TS. For example, when the length of the single TS is 1/9 that of the OFDM data block, the spectral efficiency of TDS-OFDM is 90%, which is reduced to 82% in DPN-OFDM. Therefore, to achieve high spectral efficiency and good performance over fast fading channels at the same time is really challenging for the currently available OFDM-based transmission schemes, including CP-OFDM, ZP-OFDM, TDS-OFDM, cyclic postfix OFDM, and DPN-OFDM.

The motivation of this paper is to address the aforementioned technical challenges by proposing a fundamentally distinct OFDM transmission scheme called time-frequency training OFDM (TFT-OFDM), which achieves high spectral efficiency as well as reliable performance in high speed mobile environments. The innovation and contribution of this paper can be specifically described as below: 1) Unlike TDS-OFDM or CP-OFDM where the training information exists only in the time or frequency domain, TFT-OFDM has training information in both time and frequency domains for every TFT-OFDM symbol, i.e., TFT-OFDM has TS in the time domain and a very small amount of grouped pilots in the frequency domain; 2) Unlike TDS-OFDM or CP-OFDM where the channel estimation is solely dependent on either time-domain TS or frequency-domain pilots, the proposed joint time-frequency channel estimation for TFT-OFDM utilizes the time-domain TS to merely estimate the path delay information of the wireless channel, while the channel path coefficients are acquired by using the frequency-domain grouped pilots; 3) Unlike the IBI caused by the OFDM data block to the TS has to be cancelled completely to achieve good channel estimation in TDS-OFDM, it is not necessary to remove such interference in TFT-OFDM since the received "contaminated" TS is only used to estimate the channel's path delay information. Thus, the conventional iterative algorithm with high complexity and poor performance over fading channels can be avoided, leading to the reliable performance of TFT-OFDM in high speed mobile environments; 4) Unlike CP-OFDM where large amount of frequency-domain pilots are required, the grouped pilots used to estimate the channel path coefficients only occupy about 3% of the total subcarriers in TFT-OFDM, thus high spectral efficiency can be also achieved.

The remainder of this paper is organized as follows. The TFT-OFDM system model is presented in Section II. The corresponding receiver design including joint time-frequency channel estimation and channel equalization is addressed in Section III. Section IV gives the performance analysis of the TFT-OFDM scheme. Simulation results are provided in Section V, and the final conclusions are drawn in Section VI.

Notation: We use the boldface letters to denote matrices and column vectors; $\mathbf{I}_N$ is the $N \times N$ identity matrix, and $\mathbf{0}_{M\times N}$ denotes the $M \times N$ zero matrix; $\mathbf{F}_N$ denotes the normalized $N \times N$ fast Fourier transform (FFT) matrix whose $(n+1, k+1)$th entry being $\exp(-j2\pi nk/N)/\sqrt{N}$; $\otimes$ presents the circular correlation, and $\odot$ means the Hadamard product of two vectors; $(\cdot)^*$, $(\cdot)^{\mathrm{T}}$, $(\cdot)^H$, $(\cdot)^{-1}$ and $|\cdot|$ denote the complex conjugate, transpose, Hermitian transpose, matrix inversion and absolute operations, respectively; $\mathrm{diag}\{\mathbf{u}\}$ means a diagonal matrix where the elements of $\mathbf{u}$ are placed at the diagonal positions; $(\cdot)_N$ presents the modulo-N operation; Finally, $\widehat{x}$ stands for the estimate of x.

II. TFT-OFDM System Model

In this section, the basic concept of the proposed TFT-OFDM system is generalized at first, then the TFT-OFDM system model is outlined.

A. Basic Concept of the TFT-OFDM System

As shown in Fig. 1, the IBI from the TS to the OFDM data block and the IBI caused by the OFDM block to the TS have distinct features in TDS-OFDM. The interference caused by the TS can be completely removed if the channel estimation is perfect, since the TS is known at the receiver. In addition, this IBI can be calculated with relatively low complexity since the TS length is not large. However, the interference caused by the OFDM data block has to be calculated with high complexity, since the OFDM block length is usually large. More importantly, such interference can not be totally eliminated even when the channel estimation is ideal, because the OFDM data block is random and unknown, and perfect OFDM detection is difficult due to the noise, the ICI, the imperfect channel equalization, and so on, especially when the channel is varying fast. Therefore, the TS-based time-domain channel estimation in TDS-OFDM is not accurate over fast fading channels. Such estimation error would in turn result in the unreliable cancellation of the IBI caused by the TS, which would deteriorate the OFDM equalization performance in the

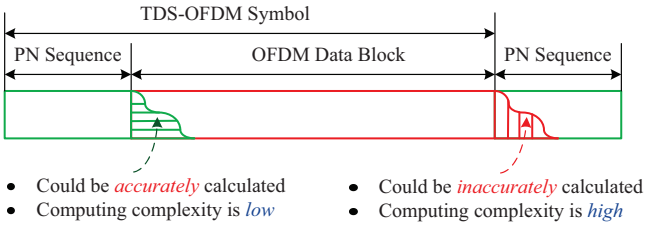

Fig. 1. Distinct features of the IBIs in TDS-OFDM.

next iteration. Consequently, the corresponding performance loss is unavoidable in TDS-OFDM.

Based on the observations that the IBI caused by the OFDM data block has to be removed for reliable channel estimation, and the complete cancellation of such IBI is difficult even when the channel estimation is perfect, TFT-OFDM is derived in this paper to provide a fundamentally distinct solution. In the proposed TFT-OFDM scheme, unlike the conventional method where both the channel path delays and the channel path coefficients are estimated by using the "clean" received TS after IBI cancellation, we do not remove the IBI imposed on the TS, but directly use the "contaminated" TS without IBI cancellation to obtain the partial channel information: the path delays of the channel, while the rest part of the channel information: the path coefficients, are acquired by utilizing the small amount of grouped pilots in the frequency domain. In this way, the IBI caused by the OFDM data block needs not to be removed, leading to the breaking of the mutually conditional relationship between the channel estimation and channel equalization in TDS-OFDM. Consequently, the iterative interference cancellation algorithm with poor performance could be avoided. The only cost is the extra frequency-domain grouped pilots, which lead to the spectral efficiency loss compared with TDS-OFDM. However, such loss is negligible, since the pilots used to estimate the path coefficients only occupy about 3% of the total subcarriers in the proposed TFT-OFDM solution.

B. TFT-OFDM System Model

Unlike TDS-OFDM or CP-OFDM where the training information only exists in the time or frequency domain, Fig. 2 shows that TFT-OFDM has training information in both time and frequency domains for every TFT-OFDM symbol, i.e., the time-domain TS and the frequency-domain grouped pilots scattered over the signal bandwidth are used in TFT-OFDM. The signal structure of the TFT-OFDM scheme can be described in the time domain and frequency domain, respectively.

In the time domain, the ith TFT-OFDM symbol $\mathbf{s}_i = [s_{i,-M} \ \cdots \ s_{i,-1} \ s_{i,0} \ s_{i,1} \ \cdots \ s_{i,N-1}]^T$ is composed of the known time-domain TS $\mathbf{c}_i = [c_{i,0} \ c_{i,1} \ \cdots \ c_{i,M-1}]^T$ and the OFDM data block $\mathbf{x}_i = [x_{i,0} \ x_{i,1} \ \cdots \ x_{i,N-1}]^T$ as below

$$\mathbf{s}_i = \begin{bmatrix} \mathbf{c}_i \\ \mathbf{x}_i \end{bmatrix}_{P\times 1} = \begin{bmatrix} \mathbf{I}_M \\ \mathbf{0}_{N\times M} \end{bmatrix}_{P\times M} \mathbf{c}_i + \begin{bmatrix} \mathbf{0}_{M\times N} \\ \mathbf{I}_N \end{bmatrix}_{P\times N} \mathbf{F}_N^H \mathbf{X}_i, \tag{1}$$

where M is the length of the TS, N is the length of the OFDM data block, $P = M + N$ presents the length of the TFT-OFDM symbol, $\mathbf{X}_i = [X_{i,0} \ X_{i,1} \ \cdots \ X_{i,N-1}]^T$ denotes

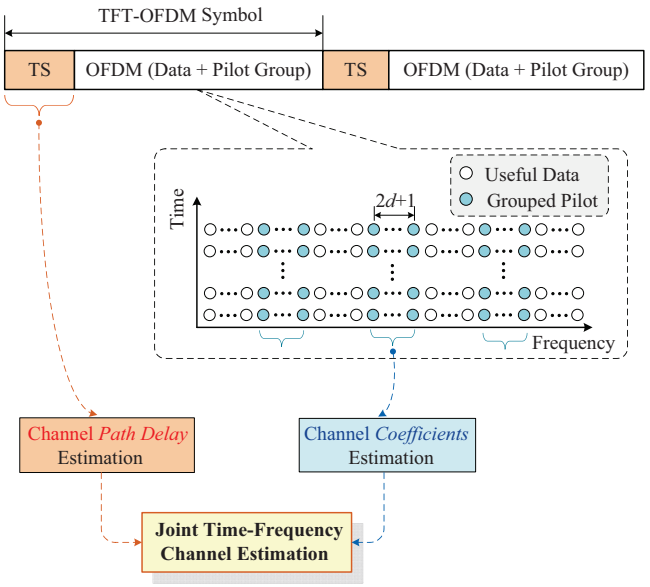

Fig. 2. Proposed signal structure and the corresponding joint time-frequency channel estimation of the TFT-OFDM scheme.

the frequency-domain OFDM symbol, and $\mathbf{x}_i = \mathbf{F}_N^H \mathbf{X}_i$. Being different from the time-domain PN sequence used in TDS-OFDM, the TS in TFT-OFDM could be any kind of sequences with desirable specific features defined in the time or frequency domain. Normally, the sequences with perfect or good autocorrelation property are preferred for channel estimation, e.g., the constant amplitude zero auto-correlation (CAZAC) sequence with constant envelop in both time and frequency domains [20], or the PN sequence used in TDS-OFDM [9]. Here we use the TS having constant envelope in the frequency domain, i.e., $\mathbf{c}_i = \mathbf{F}_M^H \mathbf{C}_i$, where $\mathbf{C}_i = [C_{i,0} \ C_{i,1} \ \cdots \ C_{i,M-1}]^T$ with the entry $|C_{i,k}| = c$, and c is an arbitrary real number. For simplicity, $C_{i,k} = \pm 1$ is used throughout this paper. It can be proved that such TS with any length has perfect circular autocorrelation property, since the circular correlation theorem [21] allows

$$\begin{aligned} \mathbf{c}_i \otimes \mathbf{c}_i &= \mathbf{F}_M^H \left(\sqrt{M} \left(\mathbf{F}_M \mathbf{c}_i \right) \odot \left(\mathbf{F}_M \mathbf{c}_i \right)^* \right) \\ &= \mathbf{F}_M^H \sqrt{M} \left(\mathbf{C}_i \odot \mathbf{C}_i^* \right) = M[1 \ \mathbf{0}_{1\times(M-1)}]^T, \end{aligned} \tag{2}$$

where $\mathbf{C}_i \odot \mathbf{C}_i^* = \mathbf{I}_{M\times 1}$ has been used.

In the frequency domain, unlike TDS-OFDM where all active subcarriers are used to carry the useful data [22], TFT-OFDM has N_d data subcarriers and N_{group} groups of binary phase-shift keying (BPSK) modulated pilots scattered over the signal bandwidth. Each pilot group has $2d + 1$ pilots. The index set of the central pilots in the N_{group} pilot groups can be denoted by $\boldsymbol{\eta} = \{\eta_0 \ \eta_1 \ \cdots \ \eta_{N_{group}-1}\}$, and the index set of all pilots is consequently presented by $\boldsymbol{\Psi} = \{\eta_0 - d \ \eta_0 - d + 1 \ \cdots \ \eta_0 + d \ \cdots \ \eta_{N_{group}-1} - d \ \cdots \ \eta_{N_{group}-1} + d\}$. The pilot number is $N_p = N_{group}(2d+1)$, and $N = N_d + N_p$. Although the frequency-domain pilots are very common in CP-OFDM systems, the grouped pilots in TFT-OFDM are different from the block-type pilots or the comb-type pilots used in most CP-OFDM systems, e.g., the second generation digital terrestrial television broadcasting system (DVB-T2) [23] and the next generation mobile wireless system called the long term

evolution (LTE) [24]. More importantly, as described later in Section III-A, TFT-OFDM requires much less pilots than CP-OFDM.

The discrete multipath channel during the ith TFT-OFDM symbol at the time instant n ($-M \le n \le N-1$) can be modeled as $\mathbf{h}_{i,n} = [h_{i,n,0}\ h_{i,n,1}\ \cdots\ h_{i,n,L-1}]^T$ of the maximum length L, where $h_{i,n,l}$ denotes the coefficient of the lth path with the delay n_l. After the cyclic prefix reconstruction of the received OFDM block has been accomplished (the hybrid domain cyclic prefix reconstruction method [25] based on the well-known overlap and add (OLA) scheme in ZP-OFDM systems [3] can be directly utilized, since TFT-OFDM is essentially equivalent to ZP-OFDM after removing the known TS at the receiver), the time-domain received OFDM block $\mathbf{y}_i = [y_{i,0}\ y_{i,1}\ \cdots\ y_{i,N-1}]^T$ is

$$\mathbf{y}_i = \mathbf{H}_i\mathbf{x}_i + \mathbf{w}_i, \tag{3}$$

where $\mathbf{w}_i$ is the additive white Gaussian noise (AWGN) vector with zero mean and covariance of $\sigma^2\mathbf{I}_N$, and the time-domain system matrix $\mathbf{H}_i$ is defined by

$$\mathbf{H}_i = \begin{bmatrix} h_{i,0,0} & 0 & \cdots & h_{i,0,2} & h_{i,0,1} \\ h_{i,1,1} & h_{i,1,0} & \cdots & h_{i,1,3} & h_{i,1,2} \\ \vdots & \vdots & \ddots & \vdots & \vdots \\ h_{i,L-1,L-1} & h_{i,L-1,L-2} & \cdots & 0 & h_{i,L-1,L-1} \\ \vdots & \vdots & \ddots & \vdots & \vdots \\ 0 & 0 & \cdots & h_{i,N-1,1} & h_{i,N-1,0} \end{bmatrix}_{N\times N} \tag{4}$$

The channel coefficient $h_{i,n,l}$ can be divided into two parts as $h_{i,n,l} = h_{i,l} + \Delta h_{i,n,l}$, where $h_{i,l} = \frac{1}{N+M}\sum_{n=-M}^{N-1} h_{i,n,l}$ denotes the average channel coefficient, and $\Delta h_{i,n,l}$ presents the channel variation compared with $h_{i,l}$. Smarmily, the system matrix $\mathbf{H}_i$ can be consequently divided into two parts as $\mathbf{H}_i = \mathbf{H}_{i,\text{ave}} + \mathbf{H}_{i,\text{var}}$, where $\mathbf{H}_{i,\text{ave}}$ is the channel "average" matrix with the (p,q)th entry being $h_{i,(p-q)_N}$, and $\mathbf{H}_{i,\text{var}}$ denotes the channel "variation" matrix with the (p,q)th entry being $\Delta h_{i,p,(p-q)_N}$. When the channel is invariant within one TFT-OFDM symbol (which is normally the assumption in TDS-OFDM due to the iterative interference cancellation method [7], [11], [12]), i.e., $h_{i,-M,l} = h_{i,-1,l} = h_{i,0,l} = \cdots = h_{i,N-1,l} = h_{i,l}$ for $0 \le l \le L-1$, we have $\Delta h_{i,n,l} = 0$, $\mathbf{H}_{i,\text{ave}}$ becomes a circular Toeplitz matrix with the first column $\mathbf{h}_i = [h_{i,0}\ h_{i,1}\ \cdots\ h_{i,L-1}]^T$, and $\mathbf{H}_{i,\text{var}} = \mathbf{0}_N$.

Using FFT to the above signal (3), we have the frequency-domain OFDM block $\mathbf{Y}_i = [Y_{i,0}\ Y_{i,1}\ \cdots\ Y_{i,N-1}]^T$ as

$$\mathbf{Y}_i = \mathbf{G}_i\mathbf{X}_i + \mathbf{W}_i, \tag{5}$$

where $\mathbf{Y}_i = \mathbf{F}_N\mathbf{y}_i$, $\mathbf{W}_i = \mathbf{F}_N\mathbf{w}_i$, and $\mathbf{G}_i$ is the $N \times N$ channel frequency response (CFR) matrix with the $(p+1, q+1)$th entry $G_{i,p,q}$ being [26]

$$G_{i,p,q} = \sum_{l=0}^{L-1}\left(\frac{1}{N}\sum_{n=0}^{N-1} h_{i,n,l}e^{-j\frac{2\pi}{N}n(p-q)}\right)e^{-j\frac{2\pi}{N}qn_l}. \tag{6}$$

If the channel is time-invariant within each TFT-OFDM symbol, the ICI coefficient $G_{i,p,q}$ ($p \ne q$) equals to zero, and $\mathbf{G}_i$ becomes a diagonal matrix. Consequently, the one-tap equalizer can be used for data detection with low complexity.

It is clear from (6) that the channel information, including the channel path delays $\{n_l\}_{l=0}^{L-1}$ as well as the path coefficients $h_{i,n,l}$, has to be obtained for data detection.

III. TFT-OFDM Receiver Design

Based on the time-frequency training information and signal structure of the TFT-OFDM scheme in Section II, this section presents the TFT-OFDM receiver design, including the joint time-frequency channel estimation, and channel equalization as well.

A. Joint Time-Frequency Channel Estimation

Unlike CP-OFDM or TDS-OFDM where the channel estimation is solely dependent on the frequency-domain pilots or the time-domain TS, whereby the path delays and path coefficients are simultaneously estimated by the time- or frequency-domain training information [7], [19], [26], [27], channel estimation in TFT-OFDM is jointly accomplished by time-frequency processing of the received TFT-OFDM signal.

1) TS-Based Path Delay Estimation

The received TS will be contaminated by the IBI from the previous OFDM data block after multi-path propagation, i.e., the received TS $\mathbf{d}_i = [d_{i,0}\ d_{i,1}\ \cdots\ d_{i,M-1}]^T$ in the ith TFT-OFDM symbol containing the contributions from the preceding $(i-1)$th unknown OFDM data block should be

$$\mathbf{d}_i = \mathbf{B}_{i,\text{ISI}}\mathbf{c}_i + \mathbf{B}_{i-1,\text{IBI}}\mathbf{x}_{i-1,N-M:N-1} + \mathbf{v}_i, \tag{7}$$

where the last M elements of $\mathbf{x}_{i-1}$ are denoted by $\mathbf{x}_{i-1,N-M:N-1}$, and the IBI caused by the previous $(i-1)$th OFDM block $\mathbf{x}_{i-1}$ is presented by $\mathbf{B}_{i-1,\text{IBI}}\mathbf{x}_{i-1,N-M:N-1}$. Note that the $M \times M$ matrices $\mathbf{B}_{i,\text{ISI}}$ and $\mathbf{B}_{i,\text{IBI}}$ can be obtained based on the "condensed" matrix $\mathbf{H}_{i,M}$ containing the first M rows and columns of the system matrix $\mathbf{H}_i$ denoted by (4). Similar to the system matrix $\mathbf{H}_i$, the "condensed" matrix $\mathbf{H}_{i,M}$ can be also divided as $\mathbf{H}_{i,M} = \mathbf{H}_{i,M,\text{ave}} + \mathbf{H}_{i,M,\text{var}}$. Since the TS length is much shorter than the TFT-OFDM symbol length, $\mathbf{H}_{i,M,\text{var}} \approx \mathbf{0}_M$ could be assumed with negligible approximation error [28]. Such error as well as the AWGN are included in the term $\mathbf{v}_i$. After that, $\mathbf{B}_{i,\text{ISI}}$ becomes the lower triangular Toeplitz matrix with the first column $\mathbf{h}_i$, and $\mathbf{B}_{i-1,\text{IBI}}$ presents the corresponding upper triangular Toeplitz matrix based on $\mathbf{B}_{i,\text{ISI}}$.

To achieve reliable channel estimation in TDS-OFDM, IBI cancellation and cyclic prefix reconstruction of the received TS are required to fully utilize the good autocorrelation property of the TS [7]

$$\begin{aligned}\mathbf{d}_{i,\text{CIR}} &= \mathbf{d}_i - \mathbf{B}_{i-1,\text{IBI}}\mathbf{x}_{i-1,N-M:N-1} + \mathbf{B}_{i,\text{IBI}}\mathbf{c}_i \\ &= \mathbf{B}_{i,\text{CIR}}\mathbf{c}_i + \mathbf{v}_i,\end{aligned} \tag{8}$$

where $\mathbf{B}_{i,\text{IBI}}\mathbf{c}_i$ denotes the "tail" caused by the transmitted TS $\mathbf{c}_i$ after the channel $\mathbf{h}_i$, $\mathbf{B}_{i,\text{CIR}}$ denotes the $M \times M$ circular matrix with the first column $\mathbf{h}_i$, and we have $\mathbf{B}_{i,\text{CIR}} = \mathbf{B}_{i,\text{ISI}} + \mathbf{B}_{i,\text{IBI}}$. Subtracting $\mathbf{B}_{i-1,\text{IBI}}\mathbf{x}_{i-1,N-M:N-1}$ in (6) means removing the IBI caused by the previous $(i-1)$th OFDM data block, while adding $\mathbf{B}_{i,\text{IBI}}\mathbf{c}_i$ indicates reconstructing the cyclic property of the received TS. Then, the

circular correlation between $\mathbf{d}_{i,\mathrm{CIR}}$ in (8) and the local TS $\mathbf{c}_i$ could achieve the complete time-domain channel estimation in TDS-OFDM [7]

$$\widetilde{\mathbf{h}}_i = \frac{1}{M}\mathbf{c}_i \otimes \mathbf{d}_{i,\mathrm{CIR}} = \frac{1}{M}\mathbf{c}_i \otimes (\mathbf{B}_{i,\mathrm{CIR}}\mathbf{c}_i + \mathbf{v}_i) = \mathbf{h}_i + \mathbf{v}_i', \quad (9)$$

where $\mathbf{v}_i' = \frac{1}{M}\mathbf{c}_i \otimes \mathbf{v}_i$ has the same statistical properties as $\mathbf{v}_i$, and the perfect autocorrelation of the TS $\mathbf{c}_i$ as shown in (2) has been used. When the PN sequence with good but not ideal autocorrelation property is used in TDS-OFDM, the estimation accuracy would be slightly lower. If the channel is varying slowly, high estimation accuracy could be iteratively achieved.

However, the channel estimation method above has two assumptions:

- *Ideal IBI removal*: Eq. (8) indicates that the IBI $\mathbf{B}_{i-1,\mathrm{IBI}}\mathbf{x}_{i-1,N-M:N-1}$ has to be completed removed from the received TS $\mathbf{d}_i$, and this requires the ideal signal detection of the previous OFDM data block $\mathbf{x}_{i-1}$ as well as the ideal estimation of the channel $\mathbf{h}_{i-1}$ in the previous TFT-OFDM symbol;
- *Perfect cyclic prefix reconstruction*: Eq. (8) also implies that, the "tail" $\mathbf{B}_{i,\mathrm{IBI}}\mathbf{c}_i$ has to be accurately estimated to achieve the reliable estimate $\widetilde{\mathbf{h}}_i$. This requires that $\mathbf{h}_i$ has already been obtained. The "tail" $\mathbf{B}_{i,\mathrm{IBI}}\mathbf{c}_i$ can be also achieved by subtracting the ith estimated OFDM block from the ith actually received OFDM block [11], or using the "tail" of the previous $(i-1)$th TS instead [12]. However, all those solutions assume perfect estimation of $\mathbf{h}_i$ or $\mathbf{h}_{i-1}$.

For the first assumption, accurate channel estimation and ideal OFDM data detection are difficult to be achieved over fast fading channels. The second supposition implies that channel estimation and cyclic prefix reconstruction are mutually conditional. Therefore, the iterative interference cancellation method has to be used in TDS-OFDM, and the performance loss is unavoidable [29].

To solve those problems, without interference cancellation, we directly use the "contaminated" TS in TFT-OFDM to obtain the rough CIR estimate $\widehat{\mathbf{h}}_i$ to merely acquire the channel path delay information

$$\widehat{\mathbf{h}}_i = \frac{1}{M}\mathbf{c}_i \otimes \mathbf{d}_i = \mathbf{h}_i + \mathbf{v}_i' + \mathbf{n}_i, \quad (10)$$

where

$$\mathbf{n}_i = \frac{1}{M}\mathbf{c}_i \otimes (\mathbf{B}_{i-1,\mathrm{IBI}}\mathbf{x}_{i-1,N-M:N-1} - \mathbf{B}_{i,\mathrm{IBI}}\mathbf{c}_i) \quad (11)$$

denotes the extra "noise" caused by the interference. However, $\mathbf{n}_i$ will not severely affect the path delay information of the roughly estimated channel $\widehat{\mathbf{h}}_i$, since the random OFDM data block $\mathbf{x}_{i-1}$ and the fixed TS $\mathbf{c}_i$ are completely uncorrelated. As an example, Fig. 3 compares the rough channel estimate $\widehat{\mathbf{h}}_i$ with the actual channel $\mathbf{h}_i$ over the Brazil D channel [30] with the signal-to-noise ratio (SNR) of 5 dB. We can observe that, although the rough estimate $\widehat{\mathbf{h}}_i$ is not accurate due to the absence of interference cancellation, the path delay information of the actual channel $\mathbf{h}_i$ is preserved well by $\widehat{\mathbf{h}}_i$, which is just the goal of this stage. Moreover, $\widehat{\mathbf{h}}_i$ in the ith

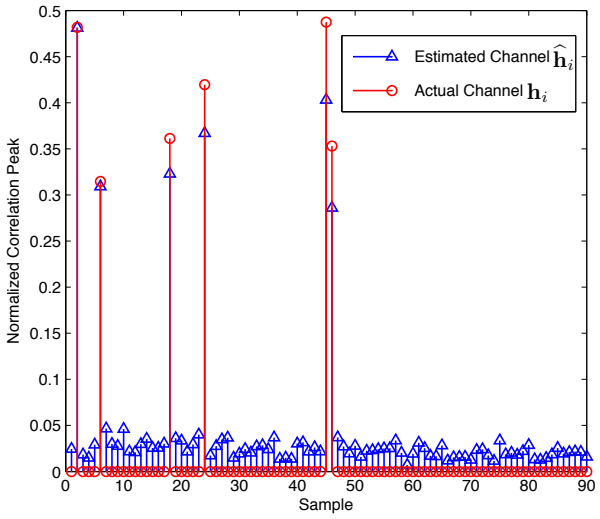

Fig. 3. Channel path delay estimation using the received time-domain TS without interference cancellation and cyclic prefix reconstruction.

TFT-OFDM symbol can be further refined by averaging the results from (10) in the preceding U TFT-OFDM symbols:

$$\overline{\mathbf{h}}_i = \frac{1}{U}\sum_{u=i-U+1}^{i}\widehat{\mathbf{h}}_u = \frac{1}{UM}\mathbf{c}_u \otimes \left(\sum_{u=i-U+1}^{i}\mathbf{d}_u\right). \quad (12)$$

Finally, the path delays of the $\mathcal{S}$ most significant taps of $\overline{\mathbf{h}}_i$ are saved in the path delay information set $\mathbf{\Gamma}$

$$\mathbf{\Gamma} = \{n_l : \left|\overline{h}_{i,n_\mathcal{S}}\right|^2 \geq P_{th}\}_{l=0}^{\mathcal{S}-1}, \quad (13)$$

where P_{th} is the predetermined power threshold, and the cardinality of $\mathbf{\Gamma}$ is $\mathcal{S}$, i.e., the channel has only $\mathcal{S}$ nonzero coefficients out of the L possible paths. Without loss of generality, $0 \leq n_0 \leq n_1 \leq \cdots \leq n_{\mathcal{S}-1} \leq L-1$ could be assumed.

It should be pointed out that, to improve the estimation accuracy of the path delay information, similar to (8), we could use the channel estimate and the detected OFDM data block in the previous $(i-1)$th TFT-OFDM symbol to calculate the removable IBI imposed on the TS in the ith TFT-OFDM symbol, and then utilize $\mathbf{B}_{i-1,\mathrm{IBI}}\mathbf{c}_i$ to approximate $\mathbf{B}_{i,\mathrm{IBI}}\mathbf{c}_i$ to accomplish the cyclic prefix reconstruction of the received TS, then the rough channel estimation can be made similar to (9). In this way, the dominant interference contaminating the TS could be removed when the SNR is low or the IBI is severe, and more reliable path delay estimation could be achieved at the cost of slightly increased receiver complexity. Note that such mechanism is essentially different from the iterative algorithm in TDS-OFDM which eliminates the IBI as completely as possible, whereas we permit the inaccuracy of the IBI removal and the existence of residual interference. Another possible simpler solution is to insert the doubled TS within several TFT-OFDM symbols, and the second received TS is used to get the relatively more reliable rough channel estimate to improve the accuracy of the path delay estimation, but this would result in the spectral efficiency loss to a certain

degree. In addition, the semi-blind approach can be also used to detect the most significant taps of the wireless channel [31].

Since the channel path delay information has been obtained in (13), the channel path coefficients should be estimated to accomplish the complete joint time-frequency channel estimation, which is the topic of the following subsection.

2) Pilot-Based Path Coefficients Estimation

For fast time-varying channels which vary even within each OFDM symbol, the nonzero path coefficients $h_{i,n,l}$ with the path delay $\mathbf{\Gamma} = \{n_l\}_{l=0}^{\mathcal{S}-1}$ can be modeled by the Q-order Taylor series expansion [27]

$$h_{i,n,l} = \boldsymbol{\theta}_n \boldsymbol{\rho}_{i,l} + \varepsilon_{i,n,l}, \tag{14}$$

where $\boldsymbol{\theta}_n = [1 \ n \ n^2 \ \cdots \ n^Q]_{1\times(Q+1)}$, $\boldsymbol{\rho}_{i,l} = [\rho_{i,l,0} \ \rho_{i,l,1} \ \cdots \ \rho_{i,l,Q}]^T_{(Q+1)\times 1}$ whose entry $\rho_{i,l,q}$ is the polynomial coefficient, and $\varepsilon_{i,n,l}$ denotes the approximation error. The order Q depends on the maximum Doppler spread f_d of the channel, i.e., the faster the channel is varying, the larger Q should be, and vice versa. According to the study in [27], $Q = 1$ ensures good approximation performance if $f_d T \leq 0.1$, where T is the OFDM block duration. Take the value $T = 500\ \mu s$ specified by Chinese national digital television standard [9] as an example, whereby the signal bandwidth is 7.56 MHz and $N = 3780$ (so we have $T = 3780/7.56 \times 10^6 = 500\ \mu s$), $f_d \leq 200$ Hz meets the criteria $f_d T \leq 0.1$. In such case, only $2\mathcal{S}$ unknown parameters are to be estimated in (14).

Since the ICI is dominantly caused by the neighboring subcarriers [32], it can be assumed that the ICI coefficient $G_{i,p,q} = 0$ if $|p - q| > d$. Thus, by substituting (14) and (6) into (5), the received frequency-domain signal $Y_{i,k}$ on the kth subcarrier can be rewritten as

$$\begin{aligned} Y_{i,k} &= G_{i,k,k}X_{i,k} + \sum_{j=0,j\neq k}^{N-1} G_{i,k,j}X_{i,j} + W_{i,k} \\ &\approx \sum_{j=k-d}^{k+d} G_{i,k,j}X_{i,j} + W_{i,k} \\ &= \sum_{n=0}^{N-1}\sum_{l=0}^{\mathcal{S}-1}\sum_{q=0}^{Q-1} \rho_{i,l,q} n^q \lambda_{i,n,l,k} + \sum_{n=0}^{N-1}\sum_{l=0}^{\mathcal{S}-1} \varepsilon_{i,n,l}\lambda_{i,n,l,k} + W_{i,k} \\ &= \sum_{n=0}^{N-1}\sum_{l=0}^{\mathcal{S}-1}\sum_{q=0}^{Q} \rho_{i,l,q} n^q \lambda_{i,n,l,k} + \zeta_{i,k}, \end{aligned} \tag{15}$$

where

$$\lambda_{i,n,l,k} = \frac{1}{N}\sum_{q=k-d}^{k+d} e^{-j\frac{2\pi}{N}n(k-q)} e^{-j\frac{2\pi}{N}qn_l} X_{i,q}, \tag{16}$$

$$\zeta_{i,k} = \sum_{n=0}^{N-1}\sum_{l=0}^{\mathcal{S}-1} \varepsilon_{i,n,l}\lambda_{i,n,l,k} + W_{i,k}. \tag{17}$$

Eq. (15) could also be expressed in the form of matrix

$$Y_{i,k} = \mathbf{\Lambda}_{i,k}\boldsymbol{\theta}_i\boldsymbol{\rho}_i + \zeta_{i,k}, \tag{18}$$

where

$$\begin{aligned} \mathbf{\Lambda}_{i,k} &= [\lambda_{i,0,0,k} \ \cdots \ \lambda_{i,0,\mathcal{S}-1,k} \ \lambda_{i,1,0,k} \ \cdots \ \lambda_{i,N-1,\mathcal{S}-1,k}]_{1\times\mathcal{S}N}, \\ \boldsymbol{\theta}_i &= [\boldsymbol{\theta}_{i,0}^T \ \boldsymbol{\theta}_{i,1}^T \ \cdots \ \boldsymbol{\theta}_{i,N-1}^T]^T_{N\mathcal{S}\times(Q+1)\mathcal{S}}, \\ \boldsymbol{\theta}_{i,n} &= [\mathrm{diag}\{\boldsymbol{\theta}_n \ \boldsymbol{\theta}_n \ \cdots \ \boldsymbol{\theta}_n\}]_{\mathcal{S}\times(Q+1)\mathcal{S}}, \\ \boldsymbol{\rho}_i &= [\boldsymbol{\rho}_{i,0}^T \ \boldsymbol{\rho}_{i,1}^T \ \cdots \ \boldsymbol{\rho}_{i,\mathcal{S}-1}^T]^T_{(Q+1)\mathcal{S}\times 1}. \end{aligned} \tag{19}$$

Using the known grouped pilots $\{X_{i,q}\}_{q=k-d}^{k+d}$ and the path delay information $\mathbf{\Gamma} = \{n_l\}_{l=0}^{\mathcal{S}-1}$ in (13), $\lambda_{i,n,l,k}$ in (16) can be calculated if $k \in \boldsymbol{\eta}$, and $\mathbf{\Lambda}_i = [\mathbf{\Lambda}_{i,\eta_0} \ \mathbf{\Lambda}_{i,\eta_1} \ \cdots \ \mathbf{\Lambda}_{i,\eta_{N_{group}-1}}]^T_{N_{group}\times\mathcal{S}N}$ is consequently known. Therefore, the received central pilots in the N_{group} frequency-domain pilot groups, i.e., $\mathbf{Y}_p = [Y_{i,\eta_0} \ Y_{i,\eta_1} \ \cdots \ Y_{i,\eta_{N_{group}-1}}]^T_{N_{group}\times 1}$, can be expressed by

$$\mathbf{Y}_p = \mathbf{\Lambda}_i\boldsymbol{\theta}_i\boldsymbol{\rho}_i + \boldsymbol{\zeta}_i = \boldsymbol{\beta}_i\boldsymbol{\rho}_i + \boldsymbol{\zeta}_i, \tag{20}$$

where $\boldsymbol{\zeta}_i = [\zeta_{i,\eta_0} \ \zeta_{i,\eta_1} \ \cdots \ \zeta_{i,\eta_{N_{group}-1}}]^T_{N_{group}\times 1}$, and $\boldsymbol{\beta}_i = \mathbf{\Lambda}_i\boldsymbol{\theta}_i$ is a matrix with size $N_{group} \times (Q+1)\mathcal{S}$.

Because $\boldsymbol{\rho}_i$ in (20) contains $(Q+1)\mathcal{S}$ unknown parameters, the pilot group number should satisfy $N_{group} \geq (Q+1)\mathcal{S}$ to guarantee the matrix $\boldsymbol{\beta}_i$ to be of full column rank. Thus, $\boldsymbol{\rho}_i$ can be estimated according to the minimum mean square error (MMSE) [33] criterion as

$$\widehat{\boldsymbol{\rho}}_i = \boldsymbol{\beta}_i^{\dagger}\mathbf{Y}_p = \left(\boldsymbol{\beta}_i^H\boldsymbol{\beta}_i + \sigma^2\mathbf{I}_{(Q+1)\mathcal{S}}\right)^{-1}\boldsymbol{\beta}_i^H\mathbf{Y}_p, \tag{21}$$

where $(\cdot)^{\dagger}$ denotes the Moore-Penrose inverse matrix, and the noise variance σ^2 can be accurately acquired by time-domain estimator using the known TS [34].

Then, $h_{i,n,l}$ in (14) can be calculated, and then $\mathbf{G}_i$ in (5) is consequently known by using $h_{i,n,l}$ in (14) and the path delays $\mathbf{\Gamma} = \{n_l\}_{l=0}^{\mathcal{S}-1}$ already obtained in (13) according to (6).

If the channel is time-invariant within one OFDM data block, i.e., the path coefficients $h_{i,n,l}$ $(0 \leq n \leq N-1)$ of the lth path are independent of the time instant n, we have

$$\widehat{h}_{i,l} = \frac{1}{N}\sum_{n=0}^{N-1}\widehat{h}_{i,n,l}, \ 0 \leq l \leq \mathcal{S}-1. \tag{22}$$

Note that only $N_p = (Q+1)(2d+1)\mathcal{S}$ pilots are required in TFT-OFDM to estimate the path coefficients after the path delay information has been obtained in (13). It has been shown that $Q = 1, d = 1$ can already provide satisfying performance over fading channels [27]. In addition, the number of the total resolvable paths $\mathcal{S}$ is usually small. For example, the six typical channel models in indoor, pedestrian, and vehicular test environments defined by the international telecommunication union (ITU) [35] have $\mathcal{S} \leq 6$ paths, the five channel models for terrestrial digital television system [30] have fewer than 6 paths. Also, [26] adopted $\mathcal{S} = 6$ and [27] assumed $\mathcal{S} = 4$. So we can assume that $\mathcal{S} = 6$ for TFT-OFDM systems without loss of generality. In this case, only $N_p = 36$ pilots are sufficient to estimate the path coefficients of the time-varying channels. If the channel is stationary within each TFT-OFDM symbol whereby no ICI will be caused, $Q = 0, d = 0$ can be used, and only $N_p = 6$ pilots will be required to estimate the channel path coefficients. However, in practical

applications, especially in SFN scenarios, the path number may be large, so we configure $\mathcal{S} = 20$ and consequently $N_p = 120$ pilots for system design with some margin. Note that this configuration could identify 120 resolvable paths if the channel varies slowly within one TFT-OFDM symbol, which is valid when the receiver is moving at relatively low speed. However, in CP-OFDM, both the path delays and path coefficients are estimated by using the frequency-domain pilots, and the Karhunen-Loeve theorem [26] requires that the pilot number should be not smaller than the CP length M [1]. Therefore, much fewer pilots are required by TFT-OFDM than CP-OFDM.

The proposed joint time-frequency channel estimation scheme also differs from the compressive sensing (CS) based channel estimation technique implemented either in the time domain [36] or in the frequency domain [37]–[39] in the following aspects: 1) Our proposal is a *linear overdetermined problem* whose solution can be uniquely determined by solving the linear equation array, while the CS-based technique is a *nonlinear underdetermined problem* whose non-unique solution can be acquired by several convex optimization strategies [40]; 2) Our proposal achieves the final CIR estimate by *two* sequential steps, i.e., the path delay estimation at first, and then the path coefficients estimation, while the CS-based technique jointly estimate the path delays and path gains in *one* step.

After the $N \times N$ channel matrix $\mathbf{G}_i$ in (5) has been obtained by the joint time-frequency channel estimation algorithm, the remained work is the channel equalization to recover the transmitted signal, which is to be addressed in the following subsection.

B. Channel Equalization

Soft-decision aided MMSE channel equalization with iterative ICI cancellation exploiting the *extrinsic* information from the soft-in soft-out (SISO) channel decoder is the widely used scheme with reliable equalization performance [41]. Here, we adopt the $\mathcal{O}(N)$-complexity equalizer with the following procedure [42]:

- *1) Initial MMSE symbol detection*: Using the MMSE detection criterion, the initial channel equalization is performed by

$$\widehat{X}_{i,k}^{(0)} = \frac{Y_{i,k}\widehat{G}_{i,k,k}^{*}}{|\widehat{G}_{i,k,k}|^2 + \sigma^2}, \quad k \notin \mathbf{\Psi}. \tag{23}$$

- *2) Soft decision based ICI cancellation for symbol re-detection*: Since the ICI is dominantly caused by the adjacent subcarriers, the transmitted signal on the kth subcarrier in the jth iteration is updated according to

$$\widehat{X}_{i,k}^{(j)} = \frac{\left(Y_{i,k} - \sum\limits_{q=k-d, q\neq k}^{k+d} \widehat{G}_{i,k,q}\widetilde{X}_{i,q}^{(j-1)}\right)\widehat{G}_{i,k,k}^{*}}{|\widehat{G}_{i,k,k}|^2 + \sigma^2}, \; k \notin \mathbf{\Psi}, \tag{24}$$

where $\widetilde{X}_{i,q}^{(j-1)}$ is the conditional mean of the qth estimated symbol $\widehat{X}_{i,q}^{(j-1)}$ generated by the soft mapper using the *a posteriori* log-likelihood ratio (LLR) and the *extrinsic* LLR provided by the soft channel decoder. Note that $\widetilde{X}_{i,q}^{(0)} = 0$ is assumed for the first iteration.

- *3) Extrinsic LLR updating*: The new estimates $\widehat{X}_{i,k}^{(j)}$ ($k \notin \mathbf{\Psi}$) are used by the soft demapper to update the *extrinsic* LLR reliability information used by the soft channel decoder, which updates the *a posteriori* LLR and the *extrinsic* LLR for the next iteration. See, e.g., [43], [44] for more details of the soft information exchange for iterative equalization.
- *4) Iteration termination*: The iterative process is stopped if the *a posteriori* LLR from the soft channel decoders converges, or the predetermined iteration number J_0 is reached. Otherwise, jump to *2)*. For simplicity, the predetermined iteration number $J_0 = 3$ is used in this paper.

It should be pointed out that, although the iterative ICI removal based channel equalization above is used in TFT-OFDM to remove the ICI over the fast fading channels, it is essentially different from the iterative IBI cancellation method in TDS-OFDM where both the channel estimation and channel equalization are involved and coupled together. If the channel can be assumed quasi-stationary during each TFT-OFDM symbol, the iterative ICI removal is not necessary any more since no significant ICI will be introduced. However, even when the channel is static, TDS-OFDM still requires the iterative IBI cancellation, whereby channel estimation and channel equalization are iteratively involved to remove the IBIs as completely as possible.

C. Brief Summary of the TFT-OFDM Receiver Design

To make a clear understanding of the working procedure of the TFT-OFDM receiver, the algorithms mentioned above are summarized as below:

1) *Step 1: TS-based path delay estimation*. Without IBI removal, the received TS is directly used to accomplish the circular correlation with the local TS to obtain the rough channel estimate $\widehat{\mathbf{h}}_i$ in (10) or $\overline{\mathbf{h}}_i$ in (12), based on which the channel path delay information $\mathbf{\Gamma} = \{n_l\}_{l=0}^{\mathcal{S}-1}$ is achieved according to (13);
2) *Step 2: Cyclic prefix reconstruction*. The OLA based hybrid-domain cyclictiy reconstruction method [25] is used for cyclic prefix reconstruction of the received OFDM, then FFT is used to obtain the frequency-domain signal $\mathbf{Y}_i$ in (5). In this step, if the receiver is just power on and no previous channel estimate can be used, $\widehat{\mathbf{h}}_i$ in (10) can be used instead. Moremore, the channel information required for cyclictiy reconstruction

[1]In CP-OFDM, to reduce the overhead caused by the pilots, it is common to assume that channel is quasi-static during several OFDM symbols, and the staggered pilot pattern is adopted to achieve the equivalent pilot insertion density. In this way, the required pilot number in each CP-OFDM symbol could be smaller than M at the cost of performance loss over fast fading channels.

TABLE I
SPECTRAL EFFICIENCY COMPARISON.

TS Length	CP-OFDM	TDS-OFDM	DPN-OFDM	TFT-OFDM
$K = N/4$	60.00%	80.00%	66.67%	77.66%
$K = N/8$	77.78%	88.89%	80.00%	86.28%
$K = N/16$	88.23%	94.12%	88.89%	91.36%

TABLE II
THE SNR LOSS DUE TO PILOT POWER BOOSTING.

Guard Interval Length	CP-OFDM	TFT-OFDM
$K = N/4$	0.77 dB	0.098 dB
$K = N/8$	0.40 dB	0.098 dB
$K = N/16$	0.21 dB	0.098 dB
$K = N/32$	0.10 dB	0.098 dB

TABLE III
THE BOOSTED PILOT POWER IN CP-OFDM AND TFT-OFDM.

Guard Interval Length	CP-OFDM	TFT-OFDM
$K = N/4$	2.50 dB	8.83 dB
$K = N/8$	2.50 dB	6.36 dB
$K = N/16$	2.50 dB	4.25 dB
$K = N/32$	2.50 dB	2.63 dB

of the i TFT-OFDM symbol can be either simply approximated by the channel estimate in the previous TFT-OFDM symbol, or predicted by the Kalman filter [45] ulitizing the temporal correlation nature of the channel as well as the channel estimates of several preceding TFT-OFDM symbols.

3) *Step 3: Joint time-frequency channel estimation*. The received central pilots $\mathbf{Y}_p$ can be selected out of $\mathbf{Y}_i$, so $\widehat{\boldsymbol{\rho}}_i$ in (21) can be acquired, then the path coefficients $\widehat{h}_{i,n,l}$ in (14) can be obtained. Consequently, the complete CFR $\mathbf{G}_i$ in (5) and $\widehat{G}_{i,p,q}$ in (6) is achieved by using the path delays $\mathbf{\Gamma} = \{n_l\}_{l=0}^{\mathcal{S}-1}$ in (13) and the path coefficients $\widehat{h}_{i,n,l}$ in (14);
4) *Step 4: Channel equalization*. Based on the CFR $\widehat{G}_{i,p,q}$, the initial symbol detection is done via (23), then the symbol re-detection with soft decision based iterative ICI cancellation can be realized by (24), whose results are then used for extrinsic information updating. Finally, the iterative ICI cancellation is terminated when the maximum iteration number J_0 is reached.

IV. PERFORMANCE ANALYSIS OF TFT-OFDM

The system performances of the proposed TFT-OFDM scheme, including the spectral efficiency, pilot power and the corresponding SNR loss, the equivalent SNR loss due to the cyclic prefix reconstruction, the receiver performance over time-varying channels, and the receiver complexity, are analyzed in this section.

A. Spectral Efficiency

One major merit of OFDM is its high spectral efficiency due to the orthogonality between the subcarriers although they are overlapped. The spectral efficiency is defined as the net bit rate over a certain signal bandwidth, i.e., the ideal OFDM system without guard interval or pilots has the spectral efficiency [46]

$$\mathrm{E}_{\mathrm{ideal}} = \frac{N\alpha/T}{N/T} = \alpha \ (\mathrm{bit/s/Hz}), \tag{25}$$

where 2^α denotes the constellation points of the modulation scheme, e.g., $\alpha = 4$ for 16QAM, $N\alpha/T$ stands for the net bit rate, and N/T is the signal bandwidth.

However, both the time-domain guard interval and the frequency-domain pilots would reduce the actual spectral efficiency of the practical OFDM systems [46]. So the spectral efficiency of TFT-OFDM is

$$\mathrm{E}_{\mathrm{real}} = \mathrm{E}_{\mathrm{ideal}} \frac{N - N_p}{M + N} \ (\mathrm{bit/s/Hz}). \tag{26}$$

When the same modulation scheme is taken into account, we define the *normalized spectral efficiency* in the form of percentage as below:

$$\mathrm{E}_0 = \frac{\mathrm{E}_{\mathrm{real}}}{\mathrm{E}_{\mathrm{ideal}}} = \frac{N - (Q+1)(2d+1)\mathcal{S}}{M+N} \times 100\%. \tag{27}$$

The key advantage of TDS-OFDM over CP-OFDM is the increased spectral efficiency since no pilot is used in TDS-OFDM, but the IBIs between the TS and the OFDM data block deteriorate the system performance over fast fading channels. The DPN-OFDM solution can solve the performance loss problem, but the doubled TS length obviously reduces the spectral efficiency. Regarding to the TFT-OFDM scheme proposed in this paper, the TS has the same length as the guard interval in TDS-OFDM and CP-OFDM systems, while only $N_p = 120$ frequency-domain grouped pilots can be configured with some design margin as discussed in Section III-A. For digital broadcasting systems like DVB-T2 [23], typically $N = 4096$ (4K mode) is used (In Chinese national digital television standard [9], $N = 3780$ is adopted), which means that the grouped pilots only occupy less than 3% of the signal bandwidth.

Table I shows the spectral efficiency comparison between CP-OFDM, TDS-OFDM, DPN-OFDM and the proposed TFT-OFDM schemes, whereby the parameter $N = 4096$ typically used by digital broadcasting systems is considered. As mentioned above, only less than 3% of the total subcarriers are used as the grouped pilots in TFT-OFDM, which is independent of the guard interval length, while CP-OFDM requires the pilot occupation ratio of 12.5% when $M = N/8$. It is clear that TFT-OFDM only subjects to negligible loss in spectral efficiency compared with TDS-OFDM who has the least overhead. It also shows that TFT-OFDM has higher efficiency than CP-OFDM and DPN-OFDM, especially when the guard interval is long, which is just the important application scenario of the single frequency network (SFN) mode for the digital broadcasting systems as well as the next generation broadband wireless system called LTE [24]. For example, TFT-OFDM has the higher spectral efficiency than CP-OFDM by about 8.5% when $M = N/8$, and TFT-OFDM outperforms DPN-OFDM by the increase of 11% in spectral efficiency when $M = N/4$.

B. Pilot Power and the Corresponding SNR Loss

In standard CP-OFDM systems, the power boosting technique [23] is commonly used to increase the average power of

the pilots to achieve more reliable channel estimation, which leads to the equivalent SNR loss at the receiver

$$\mathrm{SNR}_{\mathrm{loss}} = 10\log_{10}\left(\frac{N_p \mathrm{E}_p + (N-N_p)\,\mathrm{E}_d}{N\mathrm{E}_d}\right), \qquad (28)$$

where E_p and E_d denote the average power of the pilot and data, respectively. Such SNR loss is not negligible, especially when the pilot number is large in CP-OFDM. However, the proposed TFT-OFDM scheme only requires a small amount of grouped pilots, so the SNR loss will be small. Table II compares the SNR loss in CP-OFDM and TFT-OFDM, where the case that E_p is 2.5 dB higher than E_d as specified by DVB-T2 [23] is taken as an example. It can be found that the SNR loss in CP-OFDM is relative to the guard interval length, and 0.40 dB SNR loss will be introduced when $M = N/8$, while the negligible SNR loss in TFT-OFDM is 0.098 dB, which is independent of the guard interval length.

Furthermore, if the same SNR loss is permitted in TFT-OFDM as that in CP-OFDM, the pilot power in TFT-OFDM could be much higher than that in CP-OFDM. As shown in Table III, if the SNR loss of 0.40 dB is affordable when $M = N/8$, the boosted pilot power in TFT-OFDM could be 3.86 dB higher than that in CP-OFDM, which is beneficial for more accurate channel estimation. Due to the lower pilot occupation ratio in TFT-OFDM than CP-OFDM, the pilot power boosting technique is more efficient for more reliable channel estimation, e.g., the boosted pilot power from 2.5 dB to 3.0 dB in CP-OFDM is equivalent to the boosted pilot power from 6.36 dB to 7.20 dB in TFT-OFDM.

C. SNR Loss Due to Cyclic Prefix Reconstruction

The cyclic prefix reconstruction with the OLA method [3] would result in the noise enhancement effect caused by removing the "tail" of the OFDM data block to its head. Thus, similar to ZP-OFDM, TFT-OFDM also suffers from the SNR loss

$$\mathrm{SNR}_{\mathrm{TFT,Loss}} = 10\log_{10}\left(\frac{M+N}{N}\right). \qquad (29)$$

When $M = N/8$, the SNR loss is 0.51 dB, and when $M = N/16$, the SNR loss is 0.26 dB. Similarly, the cyclic prefix reconstruction is also required in every iteration step in TDS-OFDM, thus TDS-OFDM would sacrifice the SNR loss

$$\mathrm{SNR}_{\mathrm{TDS,Loss}} = J \cdot \mathrm{SNR}_{\mathrm{TFT,Loss}}, \qquad (30)$$

where J is the iteration number of the iterative IBI removal at the TDS-OFDM receiver. Since $J = 3$ is normally required in TDS-OFDM, the SNR loss in TFT-OFDM will be smaller than that in TDS-OFDM.

In practical applications, the maximum channel length is known according to channel path delay information set $\mathbf{\Gamma}$ in (13), and the maximum channel length $n_{\mathcal{S}}$ is usually smaller than the guard interval length M. Using this information, the noise enhancement effect could be alleviated to

$$\mathrm{SNR}'_{\mathrm{TFT,Loss}} = 10\log_{10}\left(\frac{n_{\mathcal{S}}-1+N}{N}\right). \qquad (31)$$

For example, the Vehicular B channel defined by 3GPP [35] with the maximum delay of 20 μs has the channel length of $n_{\mathcal{S}} = 152$ when the signal bandwidth is 7.56 MHz, and the SNR loss is 0.16 dB when $N = 4096$. For the AWGN channel with $n_{\mathcal{S}} = 1$, the SNR loss is 0 dB.

D. Receiver Performance over Time-Varying Channels

Compared with TDS-OFDM, TFT-OFDM could improve the receiver performance at the cost of marginally reduced spectral efficiency due to the small amount of the grouped pilots. The reasons are:

- Firstly, the iterative channel estimation and IBI cancellation in TDS-OFDM require that the channel is static within each TDS-OFDM symbol. However, the proposed TFT-OFDM receiver algorithm deals with the fast fading channel varying within every TFT-OFDM symbol, which can be also used for quasi-static channels (e.g., $Q = 0$);
- Secondly, TDS-OFDM can only obtain the channel information at the position of time-domain TS. When equalizing the OFDM data block between two adjacent TSs over fast fading channels, only the linear interpolation or other more complicated interpolation methods can be used to track the channel variation [47]. However, the proposed joint time-frequency channel estimation can accurately track the fast time-varying channel during the OFDM block by using the scattered pilots in the frequency domain.
- Thirdly, TDS-OFDM requires that the IBIs between the TS and OFDM block should be removed completely, leading to the mutually conditional relationship between channel estimation and channel equalization, and performance loss is unavoidable over fast fading channels. However, in TFT-OFDM, the joint time-frequency channel estimation is achieved by using the received "contaminated" TS without IBI cancellation and the frequency-domain grouped pilots, so the channel estimation performance is independent of the channel equalization quality.
- Finally, TFT-OFDM adopts the soft decision based ICI cancellation for symbol detection, which has better performance than the simple one-tap equalizer in TDS-OFDM.

E. Computationally Complexity

The computally complexity of the proposed scheme can be evaluated by the times of required complex complexity. Note that the soft channel decoder complexity will not be considered here, since this paper mainly focuses on channel estimation and iterative ICI removal based channel equalization. For direct yet fair comparison with the TDS-OFDM scheme adopted by Chinese digital television standard [9], we assume TFT-OFDM use the same parameters as those specified in [9], i.e., $N = 3780$, $M = 420$. When the N-point FFT/IFFT is used, the number of multiplication is $\frac{N}{2}\log_2 N$.

For CP-OFDM systems, the CFR is obtained at the pilot positions, and usually the interpolation based on discrete Fourier transform (DFT) is then used to acquire the complete CFR over the entire signal bandwidth. TDS-OFDM requires iterative receiver algorithm, and normally the iteration number is $J = 3$. DPN-OFDM utilizes the second received PN sequence to estimate the CIR, which is then converted into

TABLE IV
RECEIVER COMPLEXITY COMPARISON.

Computation	CP-OFDM	TDS-OFDM	DPN-OFDM	TFT-OFDM
Multiplication	4200	$3780J$	3780	4778740
512-FFT/IFFT	1	0	2	2
1024-FFT/IFFT	0	0	0	2
2048-FFT/IFFT	0	$4(J+1)$	0	0
3780-FFT/IFFT	2	2	2	1
8192-FFT/IFFT	0	$3(J+1)$	0	0

CFR for channel equalization. The complexity of those three conventional OFDM-based schemes are listed in Table IV.

Regarding to the proposed TFT-OFDM solution, the overall receiver procedure is summarized in Section III-C. In step 1, the 420-point circular correlation can be realized by one 512-point FFT and one 512-point IFFT [21]. In step 2, the cyclic prefix reconstruction needs one 1024-point FFT and one 1024-point IFFT to calculate the "tail" of the TS, and one 3780-point FFT is required to convert $\widetilde{\mathbf{y}}_i$ into $\mathbf{Y}_i$. In step 3, obtaining $\widehat{\boldsymbol{\rho}}_i$ in (19) needs $2N_{group}(Q+1)^2\mathcal{S}^2+(Q+1)^3\mathcal{S}^3$ times of multiplication to compute the Moore-Penrose inverse matrix of $\boldsymbol{\beta}_i$, and $N_{group}(Q+1)\mathcal{S}$ times of multiplication are used for matrix multiplication (note that computing $\boldsymbol{\Lambda}_i$ in (18) needs no multiplication, since the BPSK modulated pilots $X_{i,q}$ in (14) is the known real number). Because the ICI is dominantly caused by the adjacent $2d$ subcarriers [32], and the ICI removal in (24) also utilizes $2d$ ICI coefficients, so $(2d+1)\mathcal{S}^2N$ times of multiplication are required to calculate $\widehat{G}_{i,p,q}$ in Step 3. In step 4, the initial channel equalization needs N times of multiplication, and each ICI cancellation requires $2N(d+1)$ times of multiplication, thus $2J_0N(d+1)+N$ times of multiplication are used for channel equalization if J_0 times of iterative ICI removal are adopted (Note that the soft *extrinsic* information can be updated by the look-up table according to [43], and the complexity of channel decoder, including the calculation of LLRs, is not considered here). In summary, except the FFT/IFFT, the total number of multiplication required by the TFT-OFDM receiver is

$$M_0 = 2N_{group}(Q+1)^2\mathcal{S}^2+(Q+1)^3\mathcal{S}^3 + N_{group}(Q+1)\mathcal{S}+(2d+1)\mathcal{S}^2N+2J_0N(d+1)+N. \quad (32)$$

When the typical values discussed above are used, i.e., $N_{group}=40$, $Q=1$, $d=1$, $\mathcal{S}=20$, $J_0=3$, $N=3780$, $M=420$, the required number of multiplication is $M_0=4778740$.

It is clear from Table IV that, although the iterative ICI cancellation results in the higher complexity of TFT-OFDM than CP-OFDM and DPN-OFDM (the latter two schemes have similar complexity), the complexity of the TFT-OFDM receiver is still 63% that of the TDS-OFDM receiver.

F. Extension to Multiple-Input Multiple-Output (MIMO) Scenarios

Since the single-carrier TS occupies the whole signal bandwidth of the OFDM data block, it is known that extending TDS-OFDM to MIMO applications is difficult due to much more complicated time-domain interference than that in the single-antenna TDS-OFDM system [29], [48]. In [49] the space-time shifted TS is proposed to achieve transmit diversity for TDS-OFDM systems, but the system overhead is obviously increased, leading to the inevitable decrease in spectral efficiency. On the other hand, CP-OFDM can be easily extended to MIMO systems by adopting orthogonal pilots, at the high cost of the linearly increased pilot number with respect to the transmit antenna number N_T [24]. However, as illustrated in Fig. 4, without the obvious increase in the overhead, the proposed TFT-OFDM can be easily adapted to MIMO scenarios by configuring quasi-orthogonal time-domain TS to each transmit antenna, and using orthogonal pilots in the frequency domain. The essential idea behind the proposed TFT-OFDM solution is that, the residual IBI will not seriously affect the TS-based channel path delay estimation, so the TSs among different transmit antennas in TFT-OFDM-MIMO system need not have perfect crosscorrelation to eliminate the mutual interferences, or have ideal autocorrelation for accurate time-domain channel estimation [50]. Therefore, the TSs in TFT-OFDM-MIMO can be designed more easily than those in TDS-OFDM-MIMO. More importantly, TFT-OFDM-MIMO has much higher spectral efficiency than CP-OFDM-MIMO. Taking $N=4096, M=N/8, N_p=120, N_T=4$ as an example, we can find that 50% of the used subcarriers would be occupied by the pilots in CP-OFDM-MIMO [2], while the grouped pilots in TFT-OFDM-MIMO take up only 11.72% of the signal bandwidth.

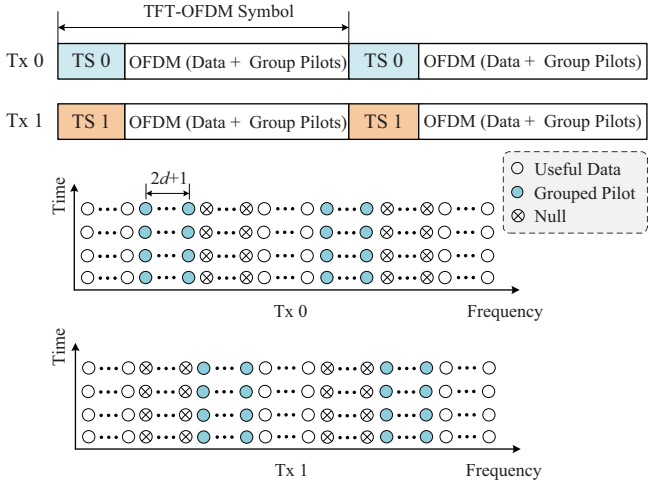

Fig. 4. Extending TFT-OFDM to MIMO applications.

V. SIMULATION RESULTS AND DISCUSSION

Simulations were carried out to investigate the performance of the proposed TFT-OFDM transmission scheme. The signal bandwidth was 7.56 MHz at the central radio frequency of 770 MHz, and the subcarrier spacing was 2 kHz. The modulation scheme 64QAM was adopted. Other system parameters were consistent with those specified in Section IV-E, e.g., $N=3780$, $M=420$, $N_{group}=40$, $Q=1$, $d=1$, $\mathcal{S}=20$, $J_0=3$. Based on the fact that nowadays almost all OFDM

[2]In practical CP-OFDM-MIMO systems like LTE, less dense pilot insertion can be used to maintain the spectral efficiency above a certain level at the cost of reduced tracking capability of the channel variation.

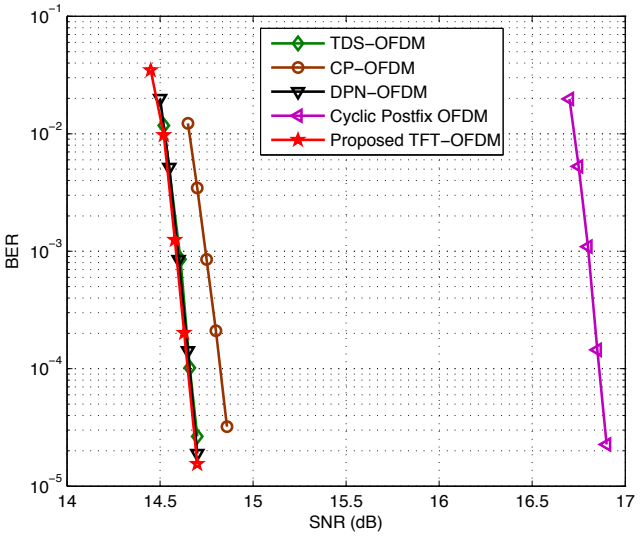

Fig. 5. BER performance comparison between the proposed TFT-OFDM scheme and the traditional schemes over the AWGN channel.

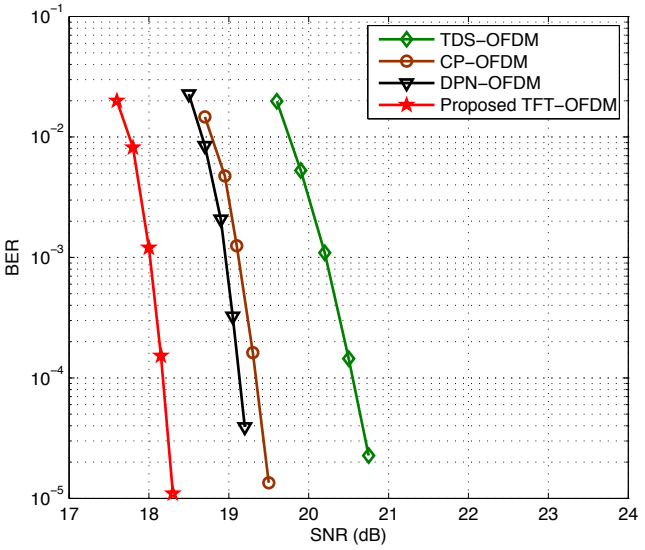

Fig. 6. BER performance comparison between the proposed TFT-OFDM scheme and three traditional schemes over the Vehicular B channel with the receiver velocity of 28 km/h.

based systems use channel coding for reliable performance, we adopted the powerful low-density parity-check (LDPC) code with the block length of 64, 8000 bits and code rate of 2/3 as specified by the standard [23]. The well-known iterative decoding algorithm called belief propagation (BP) [51] was used with the maximum iteration number of 50, whereby the soft information in each iteration could be also used for the soft decision based ICI cancellation as described in Section III-B. Two typical 6-tap multi-path channel models named Vehicular B [35] and Brazil D [30], were used. The first channel had the maximum delay spread of 20 μs, while the later one having the 0 dB echo at the delay of 5.86 μs was deeply frequency-selective characterizing the SFN environment. The maximum Doppler spread of 20 Hz and 100 Hz were considered, which corresponded to the relative receiver velocity of 28 km/h and 140 km/h @ 770 MHz, respectively.

In the simulations, we assumed M equally spaced comb-type pilots were used in CP-OFDM, since it has been proved that the such scheme could achieve the best channel estimation performance under static channels [52]. The CFR at the pilot positions were obtained at first, and then the DFT-based interpolation was used to acquire the complete CFR over the whole signal bandwidth. The classical iterative algorithm in [7] was used for TDS-OFDM. DPN-OFDM adopted the receiver algorithm proposed in [19]. The cyclic postfix OFDM used the PN sequence as the unique word [16], and the channel estimation method in [15] was used.

Fig. 5 compares the coded bit error rate (BER) performance of the conventional CP-OFDM, TDS-OFDM, DPN-OFDM, and cyclic postfix OFDM schemes with the proposed TFT-OFDM solution over the AWGN channel. The ideal channel estimation is assumed for all those systems. We can find that TFT-OFDM, TDS-OFDM and DPN-OFDM have very close BER performance, and they three have the SNR gain of 0.18 dB compared with CP-OFDM. The reason is that, the equivalent SNR at the receiver is reduced by the large amount of pilot with boosted power in CP-OFDM, and the simulation result coincides with the analysis in Section IV-B. On the other hand, the cyclic postfix OFDM scheme performs worse than other peers. For example, when the BER is 10^{-4}, the cyclic postfix OFDM performs 2.2 dB worse than TFT-OFDM. This is caused by the high average power of the redundant pilots used to generate the time-domain TS in cyclic postfix OFDM, thus the equivalent SNR at the receiver is reduced by about 2.2 dB if the same transmitted power as that in TFT-OFDM is allowed. Due to this fact, we do not consider the performance of cyclic postfix OFDM in the following parts.

Fig. 6 compares the coded BER performance of TFT-OFDM with CP-OFDM, TDS-OFDM and DPN-OFDM over the Vehicular B channel with the receiver velocity of 28 km/h. We can observe that TDS-OFDM with the highest spectral efficiency has the worst BER performance, and DPN-OFDM improves the performance at the cost of the obviously reduced spectral efficiency due to the doubled length of the TS. The performance of CP-OFDM is between that of TDS-OFDM and DPN-OFDM, while the proposed TFT-OFDM scheme has superior BER performance to those three conventional OFDM transmission schemes. For example, when the BER equals to 10^{-4}, TFT-OFDM outperforms DPN-OFDM, CP-OFDM and TDS-OFDM by the SNR gain of 0.95 dB, 1.15 dB and 2.40 dB, respectively.

Fig. 7 shows the coded BER performance comparison of those four OFDM-based transmission schemes over the Brazil D channel with the mobile speed of 140 km/h. It can be observed that TFT-OFDM still has the best performance, and the advantage has been enlarged over the fast fading channel. For example, when the BER equals to 10^{-4}, compared with DPN-OFDM, CP-OFDM and TDS-OFDM, the SNR gain achieved by TFT-OFDM is increased to be about 1.15 dB, 2.25 dB and 4.40 dB, respectively. The good BER performance over the Brazil D channel indicates that the proposed scheme

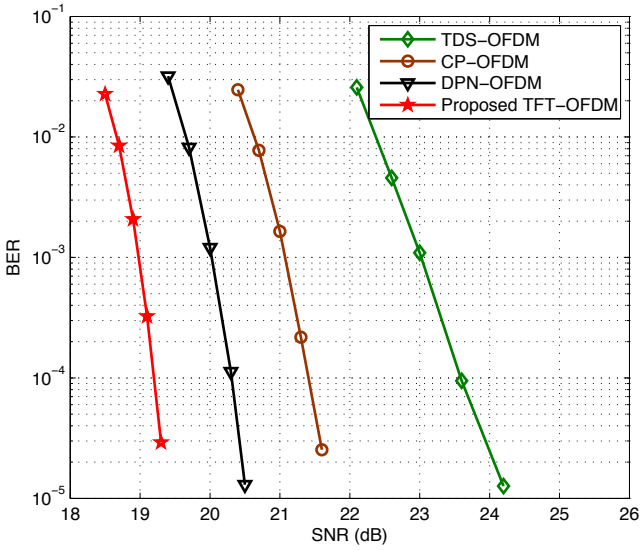

Fig. 7. BER performance comparison between the proposed TFT-OFDM scheme and three traditional schemes over the Brazil D channel with the receiver velocity of 140 km/h.

also works well in SFN scenarios. The better performance of TFT-OFDM than TDS-OFDM is mainly contributed by the avoidance of the conventional iterative interference cancellation algorithm with poor performance over fast time-varying channels. Compared with CP-OFDM and DPN-OFDM, TFT-OFDM achieves the performance improvement because the proposed joint channel estimation can accurately track the channel variation, and ICI is removed before the frequency-domain equalization.

VI. Conclusions

This paper proposes a novel OFDM-based transmission scheme called TFT-OFDM, whereby the training information exists in both time and frequency domains. The corresponding joint time-frequency channel estimation utilizes the time-domain TS without interference cancellation to estimate the channel path delays, while the channel path coefficients are acquired by using the pilot groups scattered within the OFDM symbol. In this way, the conventional iterative interference cancellation algorithm with high complexity and poor performance is avoided, and the variation of the fast fading channels within every TFT-OFDM symbol can be well tracked. The iterative ICI removal method further improves the system performance. The grouped pilots in TFT-OFDM occupy only about 3% of the signal bandwidth. Therefore, high spectral efficiency as well as good performance over fast time-varying channels could be simultaneously realized, which makes TFT-OFDM a promising physical layer transmission technique for BWC systems in high speed mobile environments. In addition, TFT-OFDM can be easily extended to MIMO and multiple access scenarios without obvious increase in the overhead. The future work is jointly exploiting the compressed sensing technique [37] and the time-frequency processing to further improve the channel estimation performance and the overall system performance for OFDM systems.

References

[1] F. Adachi and E. Kudoh, "New direction of broadband wireless technology," *Wirel. Commun. Mob. Com.*, vol. 7, no. 8, pp. 969–983, Oct. 2007.

[2] X. Yuan, Q. Guo, X. Wang, and L. Ping, "Evolution analysis of low-cost iterative equalization in coded linear systems with cyclic prefixes," *IEEE J. Sel. Areas Commun.*, vol. 26, no. 2, pp. 301–310, Feb. 2008.

[3] B. Muquet, Z. Wang, G. Giannakis, M. De Courville, and P. Duhamel, "Cyclic prefixing or zero padding for wireless multicarrier transmissions?" *IEEE Trans. Commun.*, vol. 50, no. 12, pp. 2136–2148, Dec. 2002.

[4] C. yen Ong, J. Song, C. Pan, and Y. Li, "Technology and standards of digital television terrestrial multimedia broadcasting," *IEEE Commun. Mag.*, vol. 48, no. 5, pp. 119–127, May 2010.

[5] X. Wang, P. Ho, and Y. Wu, "Robust channel estimation and ISI cancellation for OFDM systems with suppressed features," *IEEE J. Sel. Areas Commun.*, vol. 23, no. 5, pp. 963–972, May 2005.

[6] J. Wang, J. Song, and L. Yang, "A novel equalization scheme for ZP-OFDM system over deep fading channels," *IEEE Trans. Broadcast.*, vol. 56, no. 2, pp. 249–252, Jun. 2010.

[7] J. Wang, Z. Yang, C. Pan, and J. Song, "Iterative padding subtraction of the PN sequence for the TDS-OFDM over broadcast channels," *IEEE Trans. Consum. Electron.*, vol. 51, no. 11, pp. 1148–1152, Nov. 2005.

[8] J. Song, Z. Yang, L. Yang, K. Gong, C. Pan, J. Wang, and Y. Wu, "Technical review on Chinese digital terrestrial television broadcasting standard and measurements on some working modes," *IEEE Trans. Broadcast.*, vol. 53, no. 1, pp. 1–7, Feb. 2007.

[9] *Framing Structure, Channel Coding and Modulation for Digital Television Terrestrial Broadcasting System.* Chinese National Standard, GB 20600-2006, Aug. 2006.

[10] S. Zhou and G. Giannakis, "Single-carrier space-time block-coded transmissions over frequency-selective fading channels," *IEEE Trans. Inf. Theory*, vol. 49, no. 1, pp. 164–179, Jan. 2003.

[11] S. Tang, K. Peng, K. Gong, J. Song, C. Pan, and Z. Yang, "Novel decision-aided channel estimation for TDS-OFDM systems," in *Proc. IEEE International Conference on Communications (ICC'08)*, Beijing, China, May 2008, pp. 946–950.

[12] F. Yang, J. Wang, and Z. Yang, "Novel channel estimation method based on PN sequence reconstruction for Chinese DTTB system," *IEEE Trans. Consum. Electron.*, vol. 54, no. 4, pp. 1583–1588, Nov. 2008.

[13] J. Kim, S. Lee, and J. Seo, "Synchronization and channel estimation in cyclic postfix based OFDM system," in *Proc. IEEE 63rd Vehicular Technology Conference (VTC'06-Spring)*, Melbourne, Vic, May 2006, pp. 2028–2032.

[14] ——, "Synchronization and channel estimation in cyclic postfix based OFDM system," *IEICE Trans. Commun.*, vol. E90-B, no. 3, pp. 485–490, Mar. 2007.

[15] S. Tang, K. Peng, K. Gong, and Z. Yang, "Channel estimation for cyclic postfixed OFDM," in *Proc. International Conference on Communications, Circuits and Systems (ICCCAS'08)*, Fujian, China, May 2008, pp. 246–249.

[16] M. Huemer, C. Hofbauer, and J. Huber, "Unique word prefix in SC/FDE and OFDM: A comparison," in *Proc. IEEE Global Telecommunications Conference (GLOBECOM'10)*, Miami, USA, Dec. 2010, pp. 1321–1326.

[17] A. Onic and M. Huemer, "Direct vs. two-step approach for unique word generation in UW-OFDM," in *Proc. the 15th International OFDM-Workshop (InOWo'10)*, Los Alamitos, CA, Sep. 2010, pp. 145–149.

[18] C. Hofbauer, M. Huemer, and J. Huber, "On the impact of redundant subcarrier energy optimization in UW-OFDM," in *Proc. 4th International Conference on Signal Processing and Communication Systems (ICSPCS'10)*, Gold Coast, Australian, Dec. 2010, pp. 1–6.

[19] J. Fu, J. Wang, J. Song, C. Pan, and Z. Yang, "A simplified equalization method for dual PN-sequence padding TDS-OFDM systems," *IEEE Trans. Broadcast.*, vol. 54, no. 4, pp. 825–830, Dec. 2008.

[20] L. Bomer and M. Antweiler, "Perfect N-phase sequences and arrays," *IEEE J. Sel. Areas Commun.*, vol. 10, no. 4, pp. 782–789, May 1992.

[21] A. V. Oppenheim, R. Schafer, and J. Buck, *Discrete-Time Signal Processing, 4th ed.* NJ, USA: Prentice Hall, 2010.

[22] L. Dai, Z. Wang, C. Pan, and S. Chen, "Positioning in Chinese digital television network using TDS-OFDM signals," in *Proc. IEEE International Conference on Communications (ICC'11)*, Kyoto, Japan, Jun. 2011, pp. 1–5.

[23] *Frame Structure, Channel Coding and Modulation for a Second Generation Digital Terrestrial Television Broadcasting System (DVB-T2).* ETSI Standard, EN 302 755, V1.1.1, Sep. 2009.

[24] S. Sesia, I. Toufik, and M. Baker, *LTE-The UMTS Long Term Evolution: From Theory to Practice*. New Jersey, SA: John Wiley & Sons, 2009.
[25] X. Wang, H. Li, and H. Lin, "A new adaptive OFDM system with precoded cyclic prefix for dynamic cognitive radio communications," *IEEE J. Sel. Areas Commun.*, vol. 29, no. 2, pp. 431–442, Feb. 2011.
[26] W. Song and J. Lim, "Channel estimation and signal detection for MIMO-OFDM with time varying channels," *IEEE Commun. Lett.*, vol. 10, no. 7, pp. 540–542, Jul. 2006.
[27] Z. Tang, R. Cannizzaro, G. Leus, and P. Banelli, "Pilot-assisted time-varying channel estimation for OFDM systems," *IEEE Trans. Signal Process.*, vol. 55, no. 5, pp. 2226–2238, May 2007.
[28] D. Van Welden and H. Steendam, "Near optimal iterative channel estimation for KSP-OFDM," *IEEE Trans. Signal Process.*, vol. 58, no. 9, pp. 4948–4954, Sep. 2010.
[29] L. Dai, Z. Wang, and S. Chen, "A novel uplink multiple access scheme based on TDS-FDMA," *IEEE Trans. Wireless Commun.*, vol. 10, no. 3, pp. 757–761, Mar. 2011.
[30] *Digital Television Systems-Brazilian Tests-Final Report*. SET/ABERT ANATEL SP, May 2000.
[31] F. Wan, W. Zhu, and M. Swamy, "Semi-blind most significant tap detection for sparse channel estimation of OFDM systems," *IEEE Trans. Circuits Syst. I, Reg. Papers*, vol. 57, no. 3, pp. 703–713, Mar. 2010.
[32] W. Jeon, K. Chang, and Y. Cho, "An equalization technique for orthogonal frequency-division multiplexing systems in time-variant multipath channels," *IEEE Trans. Commun.*, vol. 47, no. 1, pp. 27–32, Jan. 1999.
[33] S. M. Kay, *Fundamentals of Statistical Signal Processing, Volumn I: Estimation Theory*. New Jersey, USA: Prentice-Hall, 1993.
[34] A. Ijaz, A. Awoseyila, and B. Evans, "Low-complexity time-domain SNR estimation for OFDM systems," *Electron. Lett.*, vol. 47, no. 20, pp. 1154–1156, Sep. 2011.
[35] *Guideline for Evaluation of Radio Transmission Technology for IMT-2000*. Recommendation ITU-R M. 1225, 1997.
[36] J. Haupt, W. Bajwa, G. Raz, and R. Nowak, "Toeplitz compressed sensing matrices with applications to sparse channel estimation," *IEEE Trans. Inf. Theory*, vol. 56, no. 11, pp. 5862–5875, Nov. 2010.
[37] G. Tauböck, F. Hlawatsch, D. Eiwen, and H. Rauhut, "Compressive estimation of doubly selective channels in multicarrier systems: Leakage effects and sparsity-enhancing processing," *IEEE J. Sel. Topics Signal Process.*, vol. 4, no. 2, pp. 255–271, Apr. 2010.
[38] C. Berger, S. Zhou, J. Preisig, and P. Willett, "Sparse channel estimation for multicarrier underwater acoustic communication: From subspace methods to compressed sensing," *IEEE Trans. Signal Process.*, vol. 58, no. 3, pp. 1708–1721, Mar. 2010.
[39] G. Tauböck, D. Eiwen, F. Hlawatsch, and H. Rauhut, "Compressive estimation of doubly selective channels: Exploiting channel sparsity to improve spectral efficiency in multicarrier transmissions," *IEEE J. Sel. Topics Signal Process.*, (to appear).
[40] J. A. Tropp and A. C. Gilbert, "Signal recovery from random measurements via orthogonal matching pursuit," *IEEE Trans. Inf. Theory*, vol. 53, no. 12, pp. 4655–4666, Dec. 2007.
[41] P. Schniter, "Low-complexity equalization of OFDM in doubly-selective channels," *IEEE Trans. Signal Process.*, vol. 52, no. 4, pp. 100–1011, Apr. 2004.
[42] V. Namboodiri, H. Liu, and P. Spasojevič, "Low complexity turbo equalization for mobile OFDM systems with application to DVB-H," in *Proc. IEEE Global Telecommunications Conference (GLOBECOM'10)*, Miami, USA, Dec. 2010, pp. 1328–1333.
[43] M. Tüchler, A. C. Singer, and R. Koetter., "Error equalization using a priori information," *IEEE Trans. Signal Process.*, vol. 50, no. 3, pp. 673–683, Mar. 2002.
[44] J. Huang, S. Zhou, C. Berger, and P. Willett, "Progressive inter-carrier interference equalization for OFDM transmission over time-varying underwater acoustic channels," *IEEE J. Select. Topics Signal Process.*, vol. 5, no. 8, pp. 1524–1536, Dec. 2011.
[45] C. Komninakis, C. Fragouli, A. H. Sayed, and R. D. Wesel, "Multi-input multi-output fading channel tracking and equalization using Kalman estimation," *IEEE Trans. Signal Process.*, vol. 50, no. 5, pp. 1065–1076, May 2002.
[46] X. Wang, Y. Wu, J. Chouinard, and H. Wu, "On the design and performance analysis of multisymbol encapsulated OFDM systems," *IEEE Trans. Veh. Technol.*, vol. 55, no. 3, pp. 990–1002, May 2006.
[47] X. Dong, W.-S. Lu, and A. Soong, "Linear interpolation in pilot symbol assisted channel estimation for OFDM," *IEEE Trans. Wireless Commun.*, vol. 6, no. 5, pp. 1910–1920, May 2007.
[48] Y. Zhou, Z. Pan, and H. Ye, "Prefix design for TDS-OFDM supporting frequency domain multiple access," in *Proc. 3rd International Conference on Signal Processing and Communication Systems (ICSPCS'09)*, Omaha, NE, Sep. 2009, pp. 1–5.
[49] Z. Yang, L. Dai, J. Wang, J. Wang, and Z. Wang, "Transmit diversity for TDS-OFDM broadcasting system over doubly selective fading channels," *IEEE Trans. Broadcast.*, vol. 57, no. 1, pp. 135–142, Mar. 2011.
[50] D. Sarwate, "Bounds on crosscorrelation and autocorrelation of sequences," *IEEE Trans. Inf. Theory*, vol. 25, no. 6, pp. 720–724, Nov. 1979.
[51] T. Richardson, M. Shokrollahi, and R. Urbanke, "Design of capacity-approaching irregular low-density parity-check codes," *IEEE Trans. Inf. Theory*, vol. 47, no. 2, pp. 619–637, Feb. 2001.
[52] H. Minn and N. Al-Dhahir, "Optimal training signals for MIMO OFDM channel estimation," *IEEE Trans. Wireless Commun.*, vol. 5, no. 5, pp. 1158–1168, May 2006.

Linglong Dai received his Ph.D. degree from the Department of Electronic Engineering, Tsinghua University, Beijing, China, in June 2011. He is now a Post Doctoral Fellow with the Department of Electronic Engineering as well as the Tsinghua National Laboratory of Information Science and Technology (TNList), Tsinghua University, Beijing, China. His research interests in signal processing techniques for wireless communications, with the emphasis on synchronization, channel estimation, MIMO, multiple access techniques, and wireless positioning. He has published more than ten IEEE journal/conference papers.

Zhaocheng Wang received his B.S., M.S. and Ph.D. degrees from Tsinghua University in 1991, 1993 and 1996, respectively. From 1996 to 1997, he was with Nanyang Technological University (NTU) in Singapore as a Post Doctoral Fellow. From 1997 to 1999, he was with OKI Techno Centre (Singapore) Pte. Ltd., firstly as a research engineer and then as a senior engineer. From 1999 to 2009, he worked at SONY Deutschland GmbH, firstly as a senior engineer and then as a principal engineer. He is currently a Professor at the Department of Electronic Engineering, Tsinghua University. His research areas include wireless communications, digital broadcasting and millimeter wave communications. He holds 22 granted US/EU patents and has published over 60 technical papers. He has served as technical program committee co-chair/member of many international conferences. He is a Senior Member of IEEE and a Fellow of IET.

Zhixing Yang received his B.S. degree from the Department of Electronic Engineering, Tsinghua University, Beijing, China, in 1970. He is now a full professor at the Department of Electronics Engineering of Tsinghua University, Beijing, China. He is the executive director of the State Key Laboratory on Microwave and Digital Communications, China, and the executive director of the development group of the digital television terrestrial broadcasting state standard for China. He received several national awards and held dozens of patents. His research interests are in high-speed data transmission over broadband digital television terrestrial broadcasting, wireless links, wireless communication theory and communication systems design. He is a Senior Member of IEEE.